

Acidic and catalytic properties of $\text{Cs}_x\text{H}_{3-x}\text{PW}_{12}\text{O}_{40}$ heteropolyacid compounds

Nadine Essayem^a, Gisèle Coudurier^a, Michel Fournier^b
and Jacques C. Védrine^a

^a *Institut de Recherches sur la Catalyse, CNRS, 2 avenue Albert Einstein,
F-69626 Villeurbanne Cedex, France*

^b *Laboratoire de Catalyse Hétérogène et Homogène,
Université des Sciences et Techniques de Lille, F-59655 Villeneuve d'Ascq Cedex, France*

Received 5 May 1995; accepted 17 May 1995

The heteropolyacid of Keggin structure ($\text{H}_3\text{PW}_{12}\text{O}_{40}$) and several of its cesium salts have been synthesized and characterized for their acidic properties. Chemical analysis, TGA, NH_3 adsorption–desorption and ^{31}P MAS-NMR techniques permit the characterization of the Brønsted acidity. The catalytic properties were studied for *n*-butane isomerization and for methanol conversion to dimethyl ether at 200 and 180°C, respectively. Our conclusion is that, in term of conversion, the more acidic catalysts are in the range $\text{Cs}_{2/2.7}$ if considering a wide range of acid strengths evidenced by methanol conversion. The range is $\text{Cs}_2/\text{Cs}_{2.1}$ if one considers only very strong acidity as evidenced by *n*-butane isomerization.

Keywords: cesium salts of polyoxotungstate; heteropolyacid; microporosity; acidity; *n*-butane isomerisation; methanol dehydration

1. Introduction

The heteropolyoxometallate materials have been used successfully as catalysts either in their acidic form for acid type reactions or in their cationic exchanged or substituted forms for acidic and oxidation catalytic reactions [1–6]. Among the acid forms, the most acidic corresponds to the Keggin structure $\text{H}_3\text{PW}_{12}\text{O}_{40}$ [7–10].

Such compounds exhibit very particular properties, namely their NH_4^+ , Cs^+ , K^+ , or Rb^+ salts (cations of large atomic radius) have a much higher surface area [4,11–13], a higher thermal stability [4,14] and a much lower water solubility [4,15], than their H^+ or Na^+ analogs. Another striking property, related to surface area enhancement, is that the acidic Cs^+ salts, $\text{Cs}_{3-x}\text{H}_x\text{PW}_{12}\text{O}_{40}$ exhibit much higher specific rate conversion than their H^+ analog, a fact that is at variance with what could be expected from their chemical formula. For example, Ai [14] has observed a maximum activity in catalytic dehydration of 2-propanol for the $\text{Cs}_2\text{PMo}_{12}\text{O}_{40}$

compound ($x = 2$). In contrast, the $Cs_{2.5}PW_{12}O_{40}$ compound ($x = 2.5$) was claimed to exhibit the highest activity for liquid phase reactions such as cyclohexyl acetate decomposition [16], alkylation of trimethylbenzene with cyclohexene [17] or esterification and hydrolysis reactions [18,19] and for gas phase reactions such as dimethyl ether or methanol conversion [20,21] and *n*-butane isomerization [22]. The reasons for this activity was attributed to a very high surface protonic acidity with high acid strength of the proton associated to the polyanion [4,16,21].

In this work, we have tried to elucidate some problems and particularly to discriminate between the influences of surface area and of non-exchanged protons using methanol dehydration as a “bulk-type” reaction [23,24] and isomerization of *n*-butane as a “surface-type” reaction [23,24].

2. Experimental

Pure heteropolyacid $H_3PW_{12}O_{40}$ sample was prepared in a classical way [15] including the synthesis of the sodium form and the extraction of $H_3PW_{12}O_{40}$ by diethylether.

The cesium salts were prepared by adding a CsCl solution (5 M) to an aqueous solution (0.1 M) of $H_3PW_{12}O_{40}$ with a stoichiometry corresponding to $Cs_xH_{3-x}PW_{12}O_{40}$ with $x = 3, 2.5, 2$ and 1. The precipitates were washed twice with distilled water at room temperature and separated from the liquid phase by centrifugation (4500 t min^{-1} for 30 min). The solid was finally dried by removing water, at 40°C , under reduced pressure. Chemical analysis was effected using induced coupled plasma technique for W and P elements and atomic technique for Cs.

Samples were characterized by X-ray diffraction using a Siemens diffractometer and $\text{Cu K}\alpha$ radiation and were examined by TEM with a 2010 Jeol microscope, the samples being dispersed on a microgrid from a *n*-pentane suspension.

The surface area and the pore size distribution were determined by N_2 adsorption at -196°C . The samples were outgassed 2 h at 300°C under vacuum before measurements. The pore size distribution, in the microporosity range, was calculated according to the MP method using *t*-curves [25]. Thermal analyses (TGA and DTA) were carried out, under nitrogen flow, with a Setaram 92-12 apparatus.

Ammonia adsorption and desorption experiments were performed with a home made equipment described elsewhere [26], NH_3 being analyzed by catharometry and quadrupole mass spectrometry. NH_3 1% vol/vol in argon was used. This setup allows us to identify qualitatively and quantitatively the eluted compounds. The samples were treated 2 h at 300°C under flowing nitrogen before NH_3 adsorption which was performed at 100°C .

MAS-NMR experiments were carried out with a MSL 300 Bruker spectrometer. The samples were heated at 280°C under vacuum and transferred into a zirconia holder in a glass glove box to avoid rehydration by air moisture.

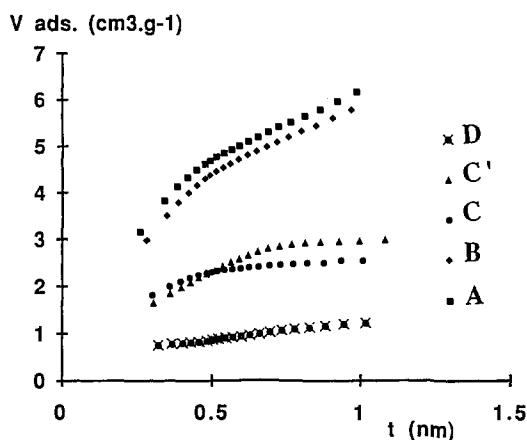


Fig. 1. t -curves of the different Cs compounds drawn from N_2 adsorption for samples: A: $Cs_3PW_{12}O_{40}$, B: $Cs_{2.7}H_{0.3}PW_{12}O_{40}$, C: $Cs_{2.1}H_{0.9}PW_{12}O_{40}$, C': $Cs_{1.9}H_{1.1}PW_{12}O_{40}$, and D: $Cs_{1.8}H_{1.2}PW_{12}O_{40}$.

Catalytic tests were performed using a differential flow microreactor in gas phase and atmospheric pressure, using 20–200 mg of catalyst, with gas chromatography analysis on line. Two reactions were chosen: (i) methanol conversion to dimethyl ether, which is sensitive to acidic properties within a rather wide range of acid strength and which is considered as a “bulk-type” reaction for heteropolyacids because of its polar nature [23,24]; (ii) n -butane isomerization to isobutane which is sensitive only to very strong acidity and is considered as a “surface-type” reaction [23,24]. Before reactions, the solids were treated 2 h at 300°C under flowing nitrogen.

3. Results and discussion

The chemical compositions of the samples are given in table 1. It clearly appears, for samples B and D, discrepancies between the chemical composition and the theoretical values drawn from the stoichiometries used for the preparation. These two samples have Cs amounts higher than expected while, in good agreement with Moffat et al. [12], sample A is slightly substoichiometric.

Note that Misono [24] has observed that the $CsH_2PW_{12}O_{40}$ salt obtained upon precipitation without washing was a mixture of $Cs_2HPW_{12}O_{40}$ salt and $H_3PW_{12}O_{40}$ which was transformed into the acidic salt $CsH_2PW_{12}O_{40}$ upon calcining at 300°C.

In our case, where washing of precipitate was performed, the composition values for B and D samples suggest that the precipitation of $Cs_3PW_{12}O_{40}$ is favored rather than that of the acidic salts $Cs_{3-x}H_xPW_{12}O_{40}$ and that washing has partly eliminated $H_3PW_{12}O_{40}$ which was not precipitated as $Cs_3PW_{12}O_{40}$ salt.

Table 1
Chemical analysis and BET surface area data

Samples	Theoretical composition	Content (wt%)			Atomic ratio		Surface area (m ² /g)
		W	P	Cs	W/Cs	Cs/P ^a	
A	Cs ₃ PW ₁₂ O ₄₀	60.0	–	10.8	4.04	2.97	147
B	Cs _{2.5} H _{0.5} PW ₁₂ O ₄₀	63.4	–	10.5	4.4	2.7	138
C	Cs ₂ HPW ₁₂ O ₄₀	65.9	–	8.4	5.7	2.1	71
C'	Cs ₂ HPW ₁₂ O ₄₀	66.4	–	7.6	6.3	1.9	72
D	CsH ₂ PW ₁₂ O ₄₀	68.1	–	7.5	6.6	1.8	26
E	H ₃ PW ₁₂ O ₄₀	67.7	0.93	0	–	0	2

^a Calculated from W/Cs ratio values taking W/P = 12 as for H₃PW₁₂O₄₀.

Two different solids corresponding to the theoretical stoichiometry Cs₂HPW₁₂O₄₀ were prepared independently (catalysts C and C'). The chemical analysis and the BET surface data are very close, which shows that our preparation procedure is rather reproducible. Note that, surprisingly, Okuhara et al. [21] found much lower surface area for all cesium samples except for Cs_{2.5}H_{0.5}PW₁₂O₄₀ and Cs₃PW₁₂O₄₀.

XRD patterns shown in fig. 2 clearly indicate that one has the cubic phase for all Cs compounds with the same unit cell, $a_0 = 1.184$ nm, in good agreement with previous data [27–29]. These results may indicate the presence of one unique crystalline Cs phase which is likely to be Cs₃PW₁₂O₄₀. However, it is to be noted that the peaks are broad, which means that the presence of intimately mixed microcrystalline cubic H₃PW₁₂O₄₀ phase of which the unit cell parameter ($a_0 = 1.216$ nm) is very close to that of Cs₃PW₁₂O₄₀ cannot be ruled out.

From X-ray peaks broadening, one may calculate the average size of the microcrystalline domains using Scherrer's relationship. For all the cesium compounds, the average sizes vary from 9 to 14 nm whatever the diffraction planes and particularly the (110) and (222) planes, which is coherent with a spherical shape of the crystalline domains. Note that the relative intensity of the peaks relative to the planes (110) and (222) was considered as a measure of microporosity by Moffat et al. [30]. In our case, the relative intensity I_{110}/I_{222} is equal to 0.25 for all cesium samples although the microporosity varies from one sample to others as shown below.

By TEM, the samples, A, B, and C appear in the form of fine particles and of spongy agglomerates, composed of fine particles. The size of the fine particles varies between 6 and 15 nm and that of the agglomerates between 50 and 300 nm. Decreasing the Cs content from samples A to C results in no striking difference, only a more compact stacking of fine particles without modification of their size. Such a morphology was already described for Cs₃PW₁₂O₄₀ [11,31].

Using the MP method derived from t -curves in N₂ adsorption measurements, one can calculate the surface of the micropores. The experimental data are given in table 2 and the t -curves in fig. 1.

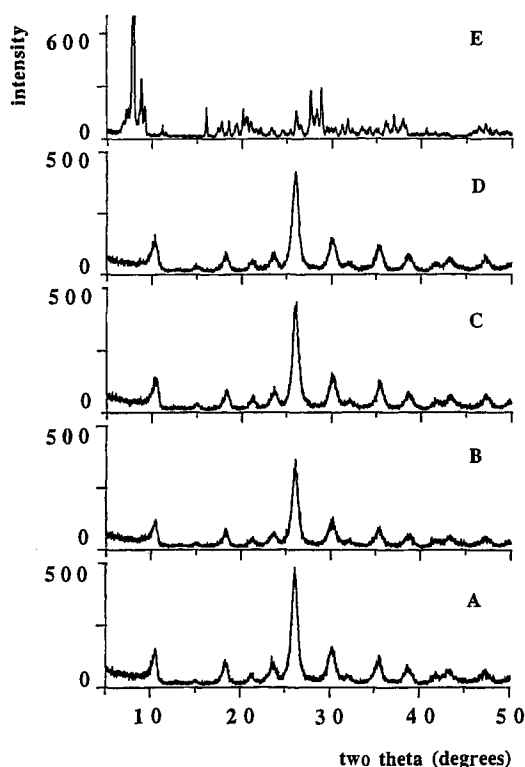


Fig. 2. XRD patterns of the different samples in their hydrated form. A: $Cs_3PW_{12}O_{40}$, B: $Cs_{2.7}H_{0.3}PW_{12}O_{40}$, C: $Cs_{2.1}H_{0.9}PW_{12}O_{40}$, D: $Cs_{1.8}H_{1.2}PW_{12}O_{40}$, and E: $H_3PW_{12}O_{40} \cdot nH_2O$.

It can be noted that for the D sample, the contribution of ultramicroporosity to the total surface area is rather high: 60% against about 30% for the others. The solids C and C', prepared with the same stoichiometry $Cs/P = 2$ present mainly ultramicropores and micropores. Nevertheless, we can observe a slight difference

Table 2
Textural features drawn from N_2 adsorption (MP method)

Samples	BET surface area ($m^2 g^{-1}$)	Surface area ($m^2 g^{-1}$)		
		ultramicroporosity (pore diameter < 0.6 nm)	microporosity (pore diameter = 0.6–1.8 nm)	mesoporosity (pore diameter > 3.6 nm)
A	147	41	60	46
B	138	46	48	44
C	71	21	43	7.3
C'	72	13	51	8
D	26	16	—	10
E	2.2	—	—	—

in their micropore size distribution: higher contribution of ultramicropores to the surface area for solid C. For the solids A and B, prepared with the highest Cs/P ratios, mesoporosity increases. It is worth noting that, depending on the Cs/ $H_3PW_{12}O_{40}$ ratio of the synthesis, we have obtained two types of compounds (C or C' and D) with about the same chemical composition, $Cs_2HPW_{12}O_{40}$ (table 1), but with different textural features (table 2).

In order to determine the number of acid Brønsted sites several experiments have been performed, namely thermogravimetric analysis, ammonia adsorption and thermodesorption and ^{31}P MAS-NMR. All the results are summarized in table 3.

For cesium salts, two water losses were observed by TGA as shown in fig. 3. Assuming the typical thermogram interpretation for 12-tungstophosphoric acid [32], they were ascribed as follows: the first loss, before 150°C for the solids A, B and before 200°C for the solids C, D, corresponds to the departure of physisorbed water and/or crystallization water. It is noteworthy that the water was removed more slowly from samples C and D. By comparison with the $H_3PW_{12}O_{40}$ thermogram, and considering their textural features, we can suggest that this slower dehydration could be due to the departure of crystallization water from a hydrated $H_3PW_{12}O_{40}$ form or of physisorbed water entrapped in ultramicropores. These losses, expressed as H_2O molecules per Keggin unit, correspond respectively to 7.6, 6.3, 6.8, 10.5 and 7.2 H_2O , for samples A, B, C, C' and D against 19.5 H_2O for $H_3PW_{12}O_{40}$.

The second water loss, occurring between 350 and 550°C is ascribed to the deprotonation process, as already observed for $H_3PW_{12}O_{40}$ [32], and corresponds respectively to 0.2, 0.33, 0.56, 0.52 and 0.57 H_2O for samples A, B, C, C' and D against 1.6 H_2O for $H_3PW_{12}O_{40}$. In terms of number of protons, solids C, C' and D appear equivalent. One proton per Keggin unit for solid D is an unexpected value, but corresponds actually to the result given by chemical analysis.

Ammonia TPD curves are shown in fig. 4. For Cs compounds, two peaks are observed, at about 250°C and 610–640°C, while for $H_3PW_{12}O_{40}$ only the high temperature peak is present. Note that mass spectrometry analysis shows that the low

Table 3
Acid sites determined by different techniques and expressed in mol per Keggin unit

Samples	TGA deprotonation	Chemical analysis	NH_3 desorption	NMR
A	0.4	0.03	0.33	0.26
B	0.7	0.3	0.42	0.47
C	1.1	0.9	0.84	0.52
C'	1.0	1.1	–	–
D	1.1	1.2	1.3	0.75
E	3.2	3.0	2.7	3.0 ^a

^a Theoretical value.

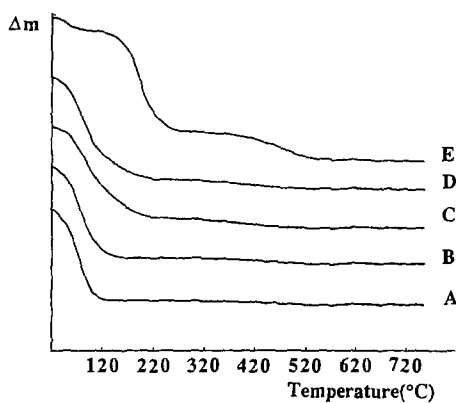


Fig. 3. Thermogravimetric variations of the different samples versus degassing temperature. A: $\text{Cs}_3\text{PW}_{12}\text{O}_{40}$, B: $\text{Cs}_{2.7}\text{H}_{0.3}\text{PW}_{12}\text{O}_{40}$, C: $\text{Cs}_{2.1}\text{H}_{0.9}\text{PW}_{12}\text{O}_{40}$, D: $\text{Cs}_{1.8}\text{H}_{1.2}\text{PW}_{12}\text{O}_{40}$, and E: $\text{H}_3\text{PW}_{12}\text{O}_{40} \cdot n\text{H}_2\text{O}$.

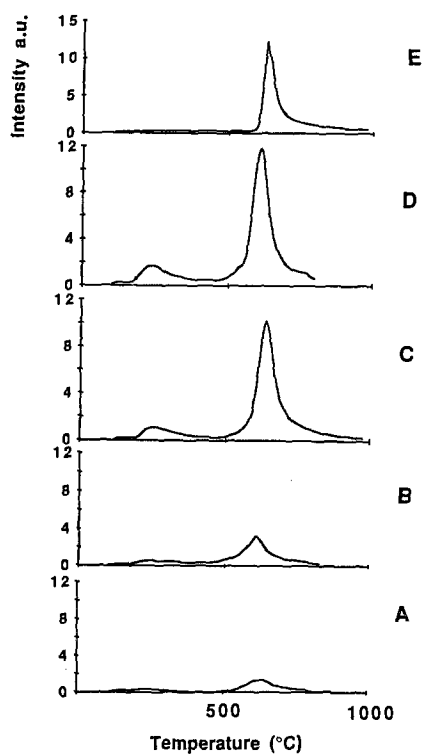


Fig. 4. Thermodesorption of NH_3 for the different samples. A: $\text{Cs}_3\text{PW}_{12}\text{O}_{40}$, B: $\text{Cs}_{2.7}\text{H}_{0.3}\text{PW}_{12}\text{O}_{40}$, C: $\text{Cs}_{2.1}\text{H}_{0.9}\text{PW}_{12}\text{O}_{40}$, D: $\text{Cs}_{1.8}\text{H}_{1.2}\text{PW}_{12}\text{O}_{40}$, and E: $\text{H}_3\text{PW}_{12}\text{O}_{40} \cdot n\text{H}_2\text{O}$. A, B, C, D: $m = 200$ mg, E: $m = 50$ mg.

temperature peak is only due to NH_3 desorption but reveals for the high temperature peak the simultaneous degassing of NH_3 , N_2 , H_2 , H_2O . The latter compound presumably arose from sample reduction by H_2 coming from NH_3 decomposition. Due to the simultaneous presence of NH_3 , N_2 and H_2 , quantitative data cannot be obtained from the catharometric peaks. However, the mass spectrometry results have permitted the estimation of both the amount of desorbed NH_3 as such and as decomposed NH_3 (taking N_2 as a probe since H_2 arising from decomposition can partly be degassed and can also reduce the sample giving rise to H_2O in addition to water coming from dehydroxylation of the samples).

The first peak at $250^\circ C$ is attributed to weakly adsorbed NH_3 . It is worth noting that this peak appears particularly for the samples C and D from which water desorbed slowly (see TGA curves). This may be due to either the desorption of NH_3 entrapped in ultramicropores or to NH_3 adsorbed on acid sites of moderate acidity which were shown to disappear with dehydration [8].

The second peak at $610\text{--}640^\circ C$ corresponds to the decomposition of the ammonium salt, $(NH_4)_3PW_{12}O_{40}$ [33,34]. This salt is formed stoichiometrically by reaction of gaseous NH_3 with the acid at $100^\circ C$ [33,34]. So, the desorption temperature cannot be used to characterize the acidity strength as one should expect from TPD experiments. Nevertheless, the total amount of ammonia desorbed at high temperature can be used as a measure of the number of protons in the different samples. Quantitative results are reported in table 3 (column 4). These values decrease with the theoretical H^+ content as expected, NH_3 being polar enough to dissolve into the whole crystallites and to neutralize all the bulk protons. However, for $Cs_3PW_{12}O_{40}$, the value is abnormally high: $0.3 H^+$ per KU against 0.03 from chemical analysis. But, it is known that the precipitation of alkaline salts of heteropolyacids is incomplete and, in ref. [12], the cesium salt $Cs_3PW_{12}O_{40}$ was shown to contain $0.1 H^+$ per KU [12]. In our work, the good agreement between TGA and NH_3 -TPD experiments suggests that the discrepancies in the H^+ content are due to a lack of precision in the chemical analysis.

The MAS-NMR technique has also been used for the characterization of the environment of the ^{31}P nucleus. The spectra measured after outgassing the samples at $280^\circ C$ are shown in fig. 5. Such a temperature was chosen from TG analysis (fig. 3) since it corresponds to the plateau ascribed to the anhydrous acid. The ^{31}P MAS-NMR spectra are composed of two peaks at -13.2 ppm and -14.6 ppm for all Cs samples. Their relative intensity depends on the Cs content. The intensity of the first peak (-13.2 ppm) follows the inverse of the Cs content and shifts to -14.9 ppm upon water adsorption. The E sample exhibits one peak near -10.6 ppm in its anhydrous form and -15.1 ppm in its hydrated form, in good agreement with literature data [35,36]. By contrast, our results for cesium salts do not agree with previous descriptions. For pure $Cs_3PW_{12}O_{40}$, only one peak at -14.9 ppm was observed [35] and for $Cs_{3-x}H_xPW_{12}O_{40}$ salts, the presence of four peaks at -10.9 , -12.1 , -13.4 and -14.9 was mentioned assigned respectively to HPA units in interaction with 3, 2, 1 or 0 H^+ [4,17,21]. The presence of several ^{31}P

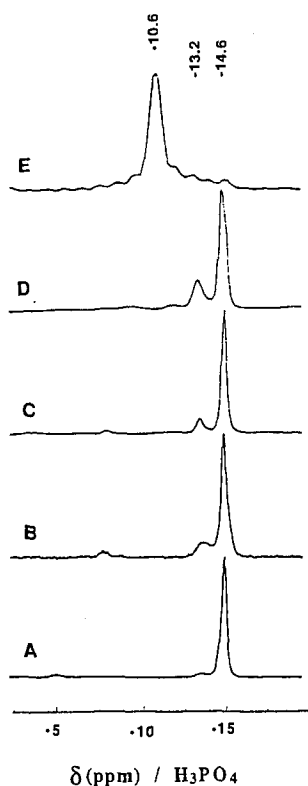


Fig. 5. MAS-NMR spectra of ^{31}P for the different samples outgassed at $280^{\circ}C$ before being transferred to the sample holder rotor in a glass box free of moisture and analysed in the following hour, at room temperature. A: $Cs_3PW_{12}O_{40}$, B: $Cs_{2.7}H_{0.3}PW_{12}O_{40}$, C: $Cs_{2.1}H_{0.9}PW_{12}O_{40}$, D: $Cs_{1.8}H_{1.2}PW_{12}O_{40}$, and E: $H_3PW_{12}O_{40} \cdot nH_2O$.

NMR peaks was also described in the case of $K_{3-x}H_xPMo_{12}O_{40}$ compounds [37] but it was attributed to the presence of an epitaxial surface layer of more or less dehydrated $H_3PMo_{12}O_{40}$ forms, dispersed on the particles of $K_3PMo_{12}O_{40}$.

In our opinion, the presence of several NMR peaks should be attributed to the presence of different structures rather than to a random distribution of protons around the Keggin units, that may lead to an average environment for the P nucleus, and therefore to an average shift, as expected for a solid solution.

Assuming that the peak at -14.6 ppm is due to the $Cs_3PW_{12}O_{40}$ pure compound, one may tentatively attribute the peak at -13.2 ppm, to a $H_3PW_{12}O_{40}$ in a partly dehydrated form entrapped in the $Cs_3PW_{12}O_{40}$ structure (since it differs from a free $H_3PW_{12}O_{40}$ dehydrated form at -10.6 ppm) which greatly depends on its environment (shift to -14.9 ppm upon hydration). According to this assumption, one can then calculate the relative amounts of entrapped $H_3PW_{12}O_{40}$ and $Cs_3PW_{12}O_{40}$ by the ratio of the -13.2 ppm peak area to the total spectrum area, namely, 8.6, 15.2, 17.1 and 25% respectively for samples A, B, C, and D. These

values correspond to 0.26, 0.45, 0.52 and 0.75 protons per Keggin unit assuming 3H for the -13.2 ppm peak and no H for the -14.6 ppm peak. In table 3, these values are compared with TGA, NH_3 -TPD and chemical composition data. The good correlation observed between the different values supports nicely our interpretation.

Catalytic results concerning isomerization of *n*-butane and dehydration of methanol are summarized in table 4. They are expressed as intrinsic and specific rates. The intrinsic values are probably reliable for *n*-butane isomerization since *n*-butane does not dissolve into the $H_3PW_{12}O_{40}$ compound while methanol or any polar compound as NH_3 , H_2O , CH_3OH , ... does dissolve at least partly in catalytic conditions [33,38,39].

For the *n*-butane isomerization reaction, the samples deactivated slowly with time on stream, which makes valid the results given after 4 min of time on stream (table 4). The selectivity to *i*-C₄ was about 90%, the other products being propane, *i*-pentane and *n*-pentane. It is noteworthy that, in term of conversion (or of specific rates), the values vary by a factor 150 between C', the most active catalyst and A the less active.

Except for the D sample, the intrinsic rates increase with the amount of bulk protons suggesting that the activity can be correlated with the amount of active sites on the surface. For the D sample, the low activity may be due to the presence of ultramicropores inaccessible to reactant.

Note, that for the same reaction but at 300°C, Na et al. [22] observed isobutane formation rates equal to 2×10^{-8} and $0.4 \times 10^{-8} \text{ mol s}^{-1} \text{ g}^{-1}$ for $Cs_{2.5}H_{0.5}PW_{12}O_{40}$ and $H_3PW_{12}O_{40}$, respectively. Such low activity values as compared to ours may be due to a too high reaction temperature (300 instead of 200°C).

Now, let us consider the methanol dehydration reaction. For this reaction, all the catalysts were stable with time on stream, except sample E which was activated

Table 4

Catalytic data for methanol conversion to dimethyl ether at 180°C and *n*-butane isomerization at 200°C after activating the sample under N_2 flow at 300°C

Samples	Rate of DME formation ^a		Rate of isobutane formation ^b	
	($10^{-8} \text{ mol s}^{-1} \text{ m}^{-2}$)	($10^{-8} \text{ mol s}^{-1} \text{ g}^{-1}$)	($10^{-8} \text{ mol s}^{-1} \text{ m}^{-2}$)	($10^{-8} \text{ mol s}^{-1} \text{ g}^{-1}$)
A	2.6	332	0.0008	0.11
B	7.4	1018	0.016	2.2
C	9.9	707	0.186	13.2
C'	—	—	0.236	16.9
D	5.4	141	0.04	1
E	204.1	430	0.737	1.6

^a Catalyst weight: 20 mg, reaction temperature = 180°C, total flow rate = 0.11 mol h^{-1} 1.5% MeOH in N_2 .

^b Catalyst weight: 300 mg, reaction temperature = 200°C, total flow rate = 0.045 mol h^{-1} 5% *n*-butane in H_2 .

during the first two hours. At 180°C, the selectivity to dimethyl ether is 100% in all cases. In contrast with the isomerization reaction, the conversion (or specific rates) varies only by a factor 7 from sample B to sample D. If the reaction was really of “bulk-type” for all the samples, the specific activity should vary with the proton content, which is not the case, the samples B and C being more active than the sample E.

We consider that, for the cesium compounds, the reaction occurs with all the superficial acid sites while the presence of an activation period for $\text{H}_3\text{PW}_{12}\text{O}_{40}$ and its high activity as compared to the superficial protonic acidity argue for the existence of a pseudoliquid phase reaction. However, as compared to the number of “bulk” protonic sites its activity is very low, which let us suppose that only some surface layers may be involved by the pseudoliquid reaction. This is in line with the observations by Nishimura et al. [39].

In contrast with the butane isomerization, sample B has the highest specific activity, as already described in the literature, and it is observed that the intrinsic activity varies only slightly for all the cesium compounds. Since for the dehydration of methanol moderate and strong acid sites are active, it may be suggested that the cesium samples contain, besides strong protonic acid sites, a large distribution of acid strength and particularly of moderate acid strength.

In view of the results in the two catalytic reactions, the main conclusions which can be reasonably drawn are as follows. For all cesium samples, the two reactions are mainly of “surface-type” while for $\text{H}_3\text{PW}_{12}\text{O}_{40}$ the C_4 isomerization is of “surface-type” and the methanol dehydration is partly of “bulk-type”. The $\text{Cs}_2\text{HPW}_{12}\text{O}_{40}$ sample (C and C') appears to be the more efficient catalyst since it contributes both by its high acid strength (determined by *n*-butane isomerization reaction) and its high surface area. This result which seems in contradiction with literature [16–22] is easily explained by the high surface area of our sample. The cesium samples, besides strong protonic acid sites, probably contain superficial sites of moderate strength which contribute to the high activity in methanol dehydration. In addition to the number of protons and to the extent of surface area, the pore distribution of the samples has to be considered in order to explain the catalysts results. Sample D shows both a medium surface area and a high number of protons. Nevertheless, the surface of this sample is majoritarily due to ultramicropores and the proton accessibility seems to be prevented. In the same way, sample C' is slightly more active than sample C. The contribution of ultramicroporosity to the surface area is lower in the case of samples C'.

The question which remains is: what is the exact nature of the cesium compounds? If they are partly exchanged salts with random distribution of protons in the structure, it is difficult to explain the formation of sample D with a substoichiometric composition, the absence of shift for the XRD peaks with the composition and the presence of only two species by ^{31}P NMR. Therefore, it is suggested that such samples correspond to the $\text{Cs}_3\text{PW}_{12}\text{O}_{40}$ salt with a given amount of highly dispersed $\text{H}_3\text{PW}_{12}\text{O}_{40}$ entrapped at the bottom of the pores and then more or less

accessible to *n*-butane or methanol molecules. Such a structure allows us to attribute the NMR peak at -13.2 ppm to partly dehydrated $H_3PW_{12}O_{40}$ species entrapped in the $Cs_3PW_{12}O_{40}$ structure.

4. Conclusion

It is confirmed that the cesium salts of $H_3PW_{12}O_{40}$ exhibit a much higher surface area than their acid analog and to show that ultramicroporosity (< 0.6 nm), microporosity (0.6 – 1.8 nm range) and mesoporosity (> 1.8 nm) are created. An enhancement of the surface area results obviously in a strong increase in specific catalytic activity. Moreover, the pore size distributions of the different $Cs_xH_{3-x}PW_{12}O_{40}$ samples are not equivalent and appear to be an important parameter.

We have also shown that the acidic features as characterized by ammonia adsorption–desorption are not simply related to the catalytic features which depend both on acidic strength and on acid site accessibility. Moreover, it is concluded that NH_3 -TPD is not a reliable technique to characterize acidic strength of heteropolyacids since the desorption temperature corresponds to the ammonium salt decomposition and not to the acid strength.

For the *n*-butane isomerization reaction, which is sensitive to very strong acid sites, the best catalysts, in term of conversion, turn out to correspond to samples with a Cs content near 2 per KU, due both to their high proton content and to their high surface area. For the methanol dehydration reaction which is sensitive to a wider range of acid strengths compared to the *n*-butane isomerization reaction, samples with Cs content between 2.7 and 2 per KU appeared to be the most efficient. Our conclusion is then that, in terms of conversion, the more acidic catalysts may be in the range $Cs_{2/2.7}$ if considering a wide range of acid strengths but rather $Cs_2/Cs_{2.1}$, if one considers only the very strong acidity.

References

- [1] I.V. Kozhevnikov and K.I. Matveev, *Appl. Catal.* 5 (1983) 135.
- [2] M. Misono, *Catal. Rev. Sci. Eng.* 29 (1987) 269.
- [3] I.V. Kozhevnikov, *Russ. Chem. Rev.* 56 (1987) 811.
- [4] M. Misono, in: *New Frontiers in Catalysis*, Proc. 10th Int. Congr. on Catalysis, Part A, eds. L. Guzzi et al. (Akadémiai Kiadó, Budapest, 1993) p. 69.
- [5] I.V. Kozhevnikov, *Russ. Chem. Rev.* 62 (1993) 473.
- [6] R.J.J. Jansen, H.M. van Veldhuizen, M.A. Schwegler and H. van Bekkum, *Recl. Trav. Chim. Pays-Bas* 113 (1994) 115.
- [7] L.C.W. Bajer and T. Pope, *J. Chem. Soc. Chem. Commun.* (1960) 1186.
- [8] A.K. Ghosh and J.B. Moffat, *J. Catal.* 101 (1986) 238.
- [9] C. Hu, M. Hashimoto, T. Okuhara and M. Misono, *J. Catal.* 143 (1993) 437.

- [10] Y. Ono, in: *Perspectives in Catalysis*, eds. J.M. Thomas and K.I. Zamaraev (Blackwells-IUPAC, London, 1992) p. 400.
- [11] N. Mizuno and M. Misono, *Chem. Lett.* (1987) 967.
- [12] G.B. McGarvey and J.B. Moffat, *J. Catal.* 128 (1991) 69.
- [13] J.L. Bonardet, J. Fraissard, G.B. McGarvey and J.B. Moffat, *J. Catal.* 151 (1995) 147.
- [14] M. Ai, *Appl. Catal.* 4 (1982) 245.
- [15] M.T. Pope, *Heteropoly and Isopolyoxometallates. Inorganic Chemistry Concepts*, Vol. 8 (Springer, Berlin, 1983).
- [16] M. Misono, *J. Catal.* 83 (1983) 121.
- [17] T. Okuhara, T. Nishimura, H. Watanabe and M. Misono, *J. Mol. Catal.* 74 (1992) 247.
- [18] Y. Izumi, M. Ono, M. Ogoya and K. Urabe, *Chem. Lett.* (1993) 825.
- [19] Y. Izumi and K. Urabe, in: *Acid-Base Catalysis II*, Stud. Surf. Sci. Catal. Vol. 90, eds. M. Hattori et al. (Elsevier, Amsterdam, 1994) p. 1.
- [20] T. Hibi, K. Takahashi, T. Okuhara, M. Misono and Y. Yoneda, *Appl. Catal.* 24 (1986) 69.
- [21] T. Okuhara, T. Nishimura, H. Watanabe, K. Na and M. Misono, in: *Acid-Base Catalysis II*, Stud. Surf. Sci. Catal., Vol. 90, eds. M. Hattori et al. (Elsevier, Amsterdam, 1994) p. 419.
- [22] K. Na, T. Okuhara and M. Misono, *Chem. Lett.* (1993) 1141.
- [23] Y. Saito, P.N. Cook, H. Hiiyama and E. Echigoya, *J. Catal.* 95 (1985) 49.
- [24] M. Misono, *Catalysis by Acids and Base*, Stud. Surf. Sci. Catal., Vol. 20, eds. B. Imelik et al. (Elsevier, Amsterdam, 1985) p. 147.
- [25] R.Sh. Mikhail, S. Brunauer and E.E. Bodor, *J. Colloid Interf. Sci.* 26 (1968) 45.
- [26] F.M.Z. Zotin, L. Tournayan, J. Varloud, V. Perrichon and R. Frety, *Appl. Catal.* 98 (1993) 99.
- [27] J.A. Santos, *Proc. Roy. Soc. A* 150 (1935) 309.
- [28] G.M. Brown, M.-R. Noe-Spirlet, W.R. Busing and H.A. Levy, *Acta Cryst. B* 33 (1977) 1038.
- [29] J.B. McMonagle and J.B. Moffat, *J. Colloid Interf. Sci.* 101 (1985) 479.
- [30] J.B. Highfield, B.K. Hodnett, J.B. McMonagle and J.B. Moffat, *Proc. 8th Int. Congr. on Catalysis*, Vol. 5, ed. IUPAC (Verlag Chemie, Frankfurt am Main, 1984) p. 611.
- [31] J. Gregg and M.M. Tayyab, *J. Chem. Soc. Faraday Trans. I* 74 (1978) 348.
- [32] M. Fournier, C. Feumi-Jantou, C. Rabia, G. Herve and S. Launay, *J. Mater. Chem.* 2 (1992) 971.
- [33] J.G. Highfield and J.B. Moffat, *J. Catal.* 88 (1984) 177.
- [34] N. Essayem, R. Fréty, G. Coudurier and J.C. Védrine, to be published.
- [35] Y. Kanda, K.Y. Lee, S. Nakata, S. Asaoka and M. Misono, *Chem. Lett.* (1989) 139.
- [36] I.V. Kozhevnikov, *Acid-Base Catalysis II*, Stud. Surf. Sci. Catal., Vol. 90, eds. M. Hattori et al. (Elsevier, Amsterdam, 1994) p. 21.
- [37] J.B. Black, N.J. Clayden, P.L. Dai, J.D. Scott, E.M. Serwicka and J.B. Goodenough, *J. Catal.* 106 (1987) 1.
- [38] T. Okuhara, T. Atai, T. Ichiki, K.Y. Lee and M. Misono, *J. Mol. Catal.* 55 (1989) 293.
- [39] T. Nishimura, T. Okuhara and M. Misono, *Chem. Lett.* (1991) 1695.